

STUDY OF FLOW AROUND A CIRCULAR CYLINDER — INFLUENCE OF NEIGHBORHOOD EFFECTS AND SEABED PROXIMITY

Leonardo L. V. Rodrigues^a and Patrícia H. Hallak^{a,b}

^a*Graduate Program in Computational Modeling, Federal University of Juiz de Fora, MG, 36036-330, Brazil, <https://www.ufjf.br/pgmc/>*

^b*Department of Applied and Computational Mechanics, Graduate Program in Computational Modeling, Federal University of Juiz de Fora, MG, 36036-330, Brazil, <http://www.ufjf.br/mac/>*

Keywords: Vortex shedding, Laminar flow, Flexible risers, Computational fluid dynamic.

Abstract. Flexible risers, widely used in offshore engineering, are long multilayer tubes designed to carry fluid — such as oil and natural gas — from the seabed to the sea platforms. In this scenario, the risers have to be able to withstand efforts ranging from their own weight, water column pressure, to dynamic loads resulting from sea currents. This study aims to evaluate the influence of sea currents on flexible risers. As for this interaction, the fluid passage was evaluated in a uniform flow around the cross-section of the tube in a two-dimensional analysis. The seasonality and variation of sea currents over time make it necessary to study different flow regimes. Therefore, a variation of Reynolds number and type of flow is applied, thus obtaining results for the laminar regime. In the flow around an obstacle is interesting the study of the vortex shedding. This phenomenon generates pressure variation on the surface structure, causing dynamic efforts that can induce oscillations, increase drag force and cause structural failure if the frequency of vortex shedding approaching one of the natural frequencies in a structure. Therefore, the drag and lift coefficients and Strouhal for Reynolds numbers in the laminar regime are so important. They are obtained through modeling using computational fluid dynamics software, ANSYS® Fluent, and then compared with the results of other models in the literature. Under the laminar regime, a study of the influence of the proximity of one riser on the other was carried out. Also, the influence of the vertical position of the riser (depth) was investigated. Thus, the force coefficients are obtained as a function of the distance from one riser to the other and the ratio of the asymmetry of the domain respectively. It can be observed that for low distances between the cylinders has a region of speed considered null, appearing as if they were not two bodies, but only one. And as the cylinders move away, that region narrows, until the second cylinder has the velocity profile similar to the first one. It could be observed that when the cylinder was in the seabed, the values of coefficients varied significantly, as did the Strouhal number.

1 INTRODUCTION

Flexible risers, widely used in offshore engineering, are long multilayer tubes designed to carry fluid — such as oil and natural gas — from the seabed to the sea platforms. In this scenario, the risers have to be able to withstand efforts ranging from their own weight, water column pressure, to dynamic loads resulting from sea currents.

This study aims to evaluate the influence of sea currents on flexible risers. As for this interaction, the fluid passage was evaluated in a uniform flow around the cross-section of the tube in a two-dimensional analysis.

It is no longer today that the study of flow around a cylinder has been the object of study for many researchers around the world. Such as Tritton (1959) and Dennis and Chang (1970) the middle of the last century with experimental and numerical work. Currently, most of the studies are done using computers, through computational techniques, such as Stringer et al. (2014), Abdulaziz (2017), and many others.

The motivation for this often comes from the cylindrical geometries used as structures and fluid transport in the offshore industry, like risers that have a circular cross-section. This use is particularly relevant due to the exploitation of new renewable energies, wind and marine energy technologies, many of which include cylindrical features that need to be assessed for their structural loading caused by vortex shedding.

1.1 Objectives

This study uses the numerical methods to solve this type of problem in the free version of ANSYS® software for a laminar flow with constant Reynolds number. The objective is to evaluate the influence of the neighborhood effect over aerodynamics coefficients when another identical cylinder is added parallel to the flow at a certain distance from the first cylinder.

Another objective is to evaluate the influence of the distance from the bed to the cylinder, which in practice can be interpreted as the proximity of the oil riser to the seabed. In this way it will evaluate what happens with the increase or decrease of these respective distances.

2 NUMERICAL METHOD

In this section a detailed account of the setup is given, including boundary, meshing strategy, solver control and post-processing. We also present some important equations for the withdrawal of data from the simulations.

2.1 Boundary conditions

The boundary conditions for the validation of the model are presented in Fig. 1. Subsequently will be presented the modification made for neighborhood effects and seabed proximity case. The domain width measures 20m and the cylinder is centralized, with a diameter equal to 0.5m.

The upstream distance since inlet until the center of cylinder is 8m and from there until the flow output has a distance of 20m. Also note that the 3rd dimension (z) was set to 1m. In order to ensure a two-dimensional analysis, there is no flow in this direction.

The outlet is just downstream of the body. A pressure boundary in this region is set to zero. When a fluid flows through a solid surface, it will come to a complete stop at the surface and the velocity relative to the surface (both normal and tangential) is assumed to be zero. This condition, where a fluid is in direct contact with a solid and “sticks” onto the surface, is commonly known as the no-slip condition (Cengel and Cimbala, 2014).

That is, the cylinder will be set to 'no-slip condition', where pressure is set to zero gradient and velocities are set to zero, $U_x = U_y = 0$. So, the upper and lower wall assigned as 'slip' boundaries, shown in Fig. 1, allow the fluid velocity component parallel to the wall to be computed, while velocity normal to the wall is set to zero, $U_y = 0$.

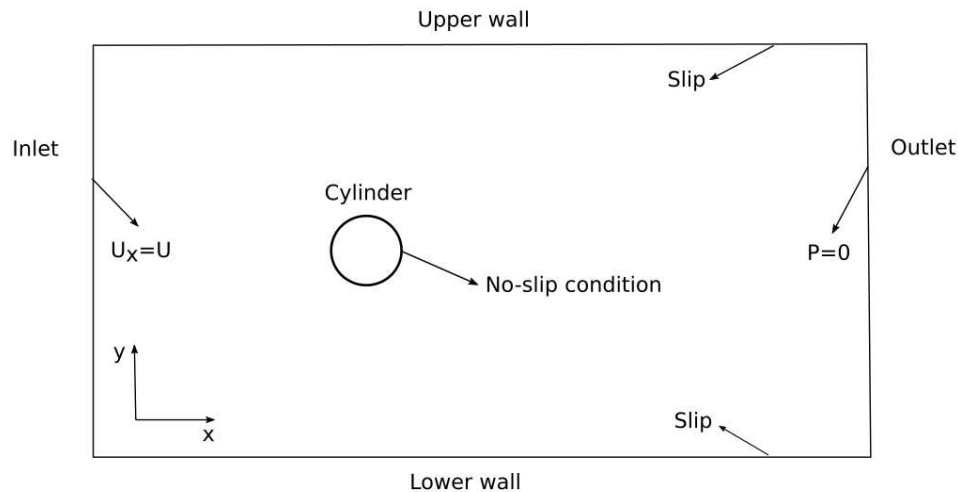


Figure 1: Schematic illustration for boundaries in laminar flow

A uniform flow is specified at the inlet, whose Reynolds number is given by Eq. (1), for flow velocity U , where ρ is the density of the fluid, D is the diameter and μ is the dynamic viscosity.

$$Re = \frac{\rho U D}{\mu} \quad (1)$$

2.2 Meshing

The template consists of a body fitted hexahedral region surrounding the cylinder with unstructured wedges filling the remaining far field domain. The mesh/grid near the cylinder is refined by modifying the grading scale and element size in the ANSYS® mesh generator. The mesh can be seen in Fig. 2. This mesh has 4220 nodes and 6295 elements.

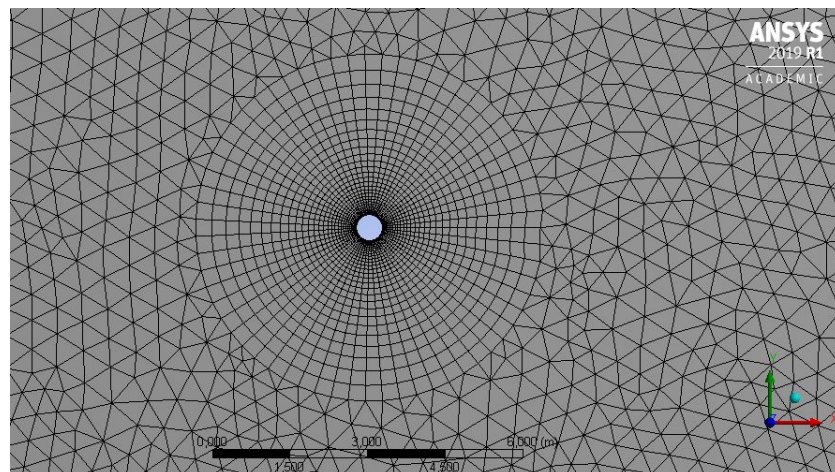


Figure 2: The visualization of the mesh

The mesh is developed so that the aspect ratio will be higher near the external domain boundaries and smaller near the cylinder.

This arrangement is made since the flow is predicted to be a developed flow on that region. The mesh around the cylinder should be finer so that it can generate more accurate results of the simulation.

2.3 Solver control

Discretization in finite volume is essential so that all equation terms can be solved. In this work the method of discretization used for gradient was least squares cell based and for the upwind scheme was second order.

The solver that is chosen for laminar transient flow simulation in ANSYS® Fluent is explicit formulation.

The result is that a low Courant number is required to maintain numerical stability of which is given in Eq. (2), where Δt is the time step and Δx is the minimum cell width. It was used Courant equal the 0.2 in all cases, since Reynolds number and mesh are same in all cases in this study.

$$Cr = \frac{U\Delta t}{\Delta x} \quad (2)$$

2.4 Post-processing

According to Blazek (2015), the force coefficients such as drag (Cd) and lift (Cl) coefficients on the cylinder could be extracted from Eq. (3), where L is the length of the pipe in z direction, F_D and F_L are drag and lift force respectively.

$$\begin{aligned} Cd &= \frac{F_D}{0.5\rho LDU^2}, \\ Cl &= \frac{F_L}{0.5\rho LDU^2}. \end{aligned} \quad (3)$$

The mean drag coefficient, \overline{Cd} and the mean lift coefficient, \overline{Cl} can be obtained from Eq. (4)

$$\begin{aligned} \overline{Cd} &= \frac{\overline{F_D}}{0.5\rho LDU^2}, \\ \overline{Cl} &= \frac{\overline{F_L}}{0.5\rho LDU^2}. \end{aligned} \quad (4)$$

The Strouhal number, could be extracted from Eq. (5), where f_v is the vortex shedding frequency in Hz.

$$St = \frac{f_v D}{U} \quad (5)$$

In this work, the value used for the velocity inlet in the x-direction U_x , was always constant and equal to $1m/s$.

The visualization of the simulation results such velocity can be seen in the ANSYS® and will be presented at the next session.

3 RESULTS AND DISCUSSION

This section will present the results obtained in this study: the comparison between the method used here with previous studies, the study of neighborhood effect and the study of seabed proximity with their respective analyzes and discussions.

3.1 Validation

To validate the model in ANSYS®[®], was chosen the case of a laminar flow on a cylinder for the Reynolds number of 100. The force coefficients, C_l and C_d as a function of time were obtained as result of the simulation and are shown in Fig. 3.

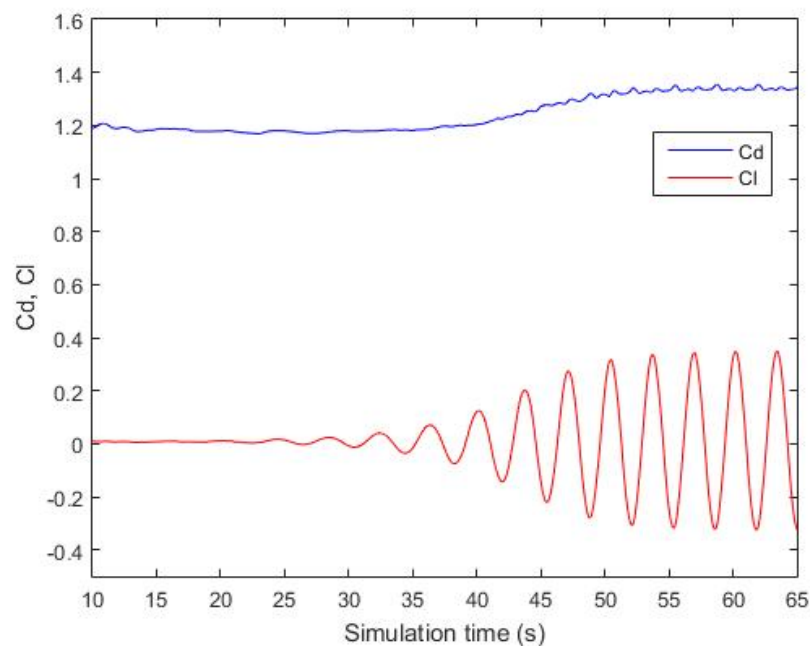


Figure 3: Hydrodynamic coefficients time histories

Table 1 shows the force coefficient obtained in this study and the results from others in the literature, where $\check{C}l$ is the lift coefficient amplitude.

Source	$\bar{C}d$	$\check{C}l$	Strouhal Number
Behr et al. (1995)	1.37	0.371	0.167
Mittal and Raghuvanshi (2001)	1.402	0.355	0.168
Berthelsen and Faltinsen (2008)	1.38	0.34	0.169
Tawekal (2015)	1.361	0.338	0.163
Previous studies	1.339	0.345	0.167

Table 1: Comparison of hydrodynamic coefficients with the previous studies

The comparison of the parameters with reference work was satisfactory. It can be make some modifications in the modeling in order to reach the objectives of this study. It was also generated the horizontal velocity profile for this simulation as follows in Fig. 4.

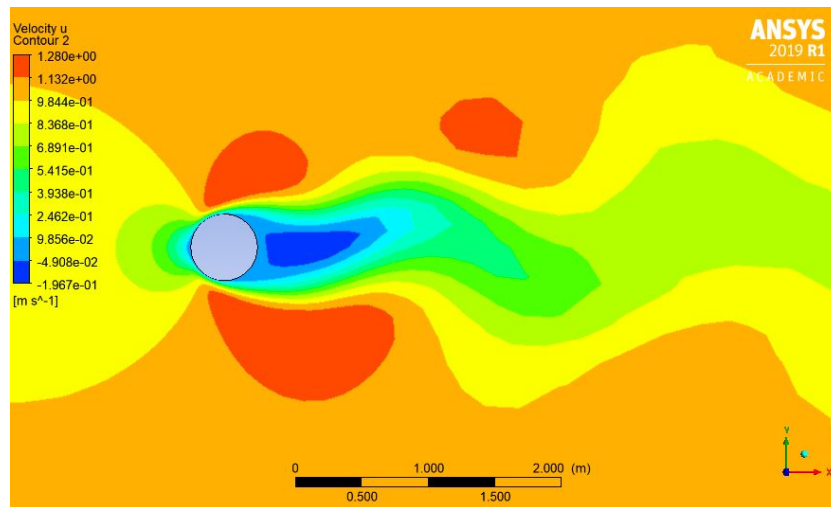


Figure 4: The visualization of horizontal velocity profile

3.2 Neighborhood effects

Under the laminar regime with Reynolds number equal to 100, a study of the influence of the proximity of one riser on the other was carried out. Thus, the force coefficients were obtained analysed as a function of the distance from one riser to the other.

The only change to the base case is the insertion of a second cylinder in the studied domain, with a distance ' e ' from the first cylinder, as indicated in the Fig. 5.

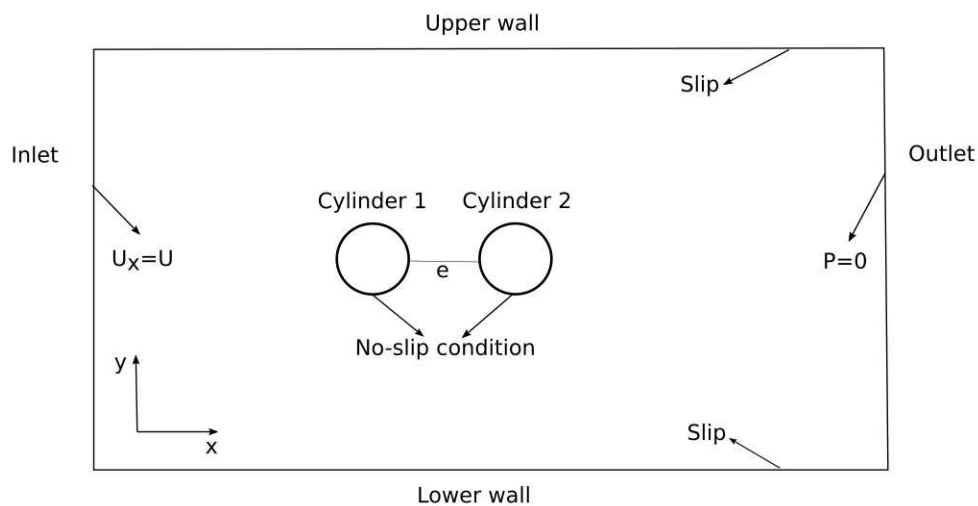


Figure 5: Schematic illustration for analyze neighborhood effects

Cases with different gap ratio (e/D) values were simulated and the results of C_d , C_l and St for each cylinders can be observed in Table 2.

The values of $\ddot{C}l_2$ and St_2 were not accounted for in the case of $e/D = 30$, as there was the occurrence of the beat phenomenon.

$e(m)$	e/D	$\overline{C}d_1$	$\overline{C}l_1$	St_1	$\overline{C}d_2$	$\overline{C}l_2$	St_2
0	0	1.16	0.006	0.13	-0.04	0.007	0.1
0.5	1	1.18	0.02	0.07	-0,07	0.002	0.05
1	2	1.15	0.002	0.1	-0.02	0.004	0.07
1.5	3	1.23	0.36	0.13	0.53	1.14	0.13
10	20	1.27	0.28	0.13	0.84	0.33	0.13
15	30	1.27	0.32	0.14	0.93	-	-
Base case		$\overline{C}d = 1.339$	$\overline{C}l = 0.345$	$St = 0.167$			

Table 2: Comparison of hydrodynamic coefficients with the distance between the cylinders

It can be observed that for low distances between the cylinders, that is, a smaller value of e has a region of speed considered null, appearing as if they were not two bodies, but only one. And as the cylinders move away, that region narrows, until the second cylinder has the velocity profile similar to the first one. It is also observed in Fig. 6 the horizontal velocities profile for such case studied is presented.

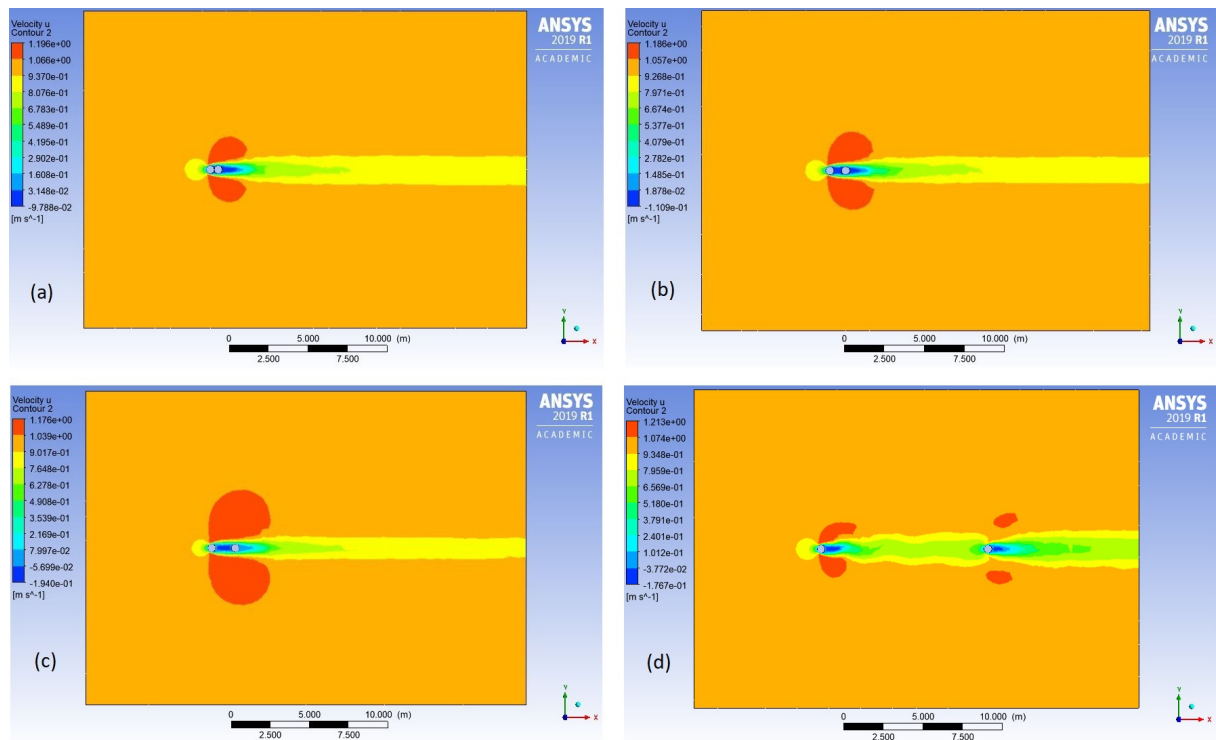


Figure 6: Horizontal velocity profile for (a) $e = 0$, (b) $e = 0.5$, (c) $e = 1$ and (d) $e = 10$

It can be observed from the Table 2 that the values of aerodynamic coefficients for the first cylinder vary slightly in relation to the base case for larger e/D . On the other hand, there is a strong variation for smaller values of e/D and this is due to the effect of the treadmill that the second cylinder causes in the first cylinder. The same behavior is not observed in cylinder 2. When the value e/D is 3, there is a sign change in the value of $\overline{C}d_2$. This indicates that from then on the bodies in fact behave as distinct.

When the distance e increases, the coefficients of the second cylinder are approaching the

value of the base case, this is due to the fact that the influence of the first cylinder in the second is tending to zero. However, the influence of the first cylinder on the second is larger than the previous case for both $\overline{C}d_2$ and $\ddot{C}l_2$. In relation to the Strouhal number, greater variations were observed for the smaller ratio e/D .

3.3 Seabed proximity

In this case the influence of the vertical position of the riser (depth) was investigated. Thus, the force coefficients were analysed through the ratio of the asymmetry of the domain.

The change to the base case is the approximation of the cylinder to the seabed. For this, the condition of the lower wall was also changed to 'No-slip condition'. Fig. 7 shows the new configuration, where j represents the distance from the cylinder to the seabed.

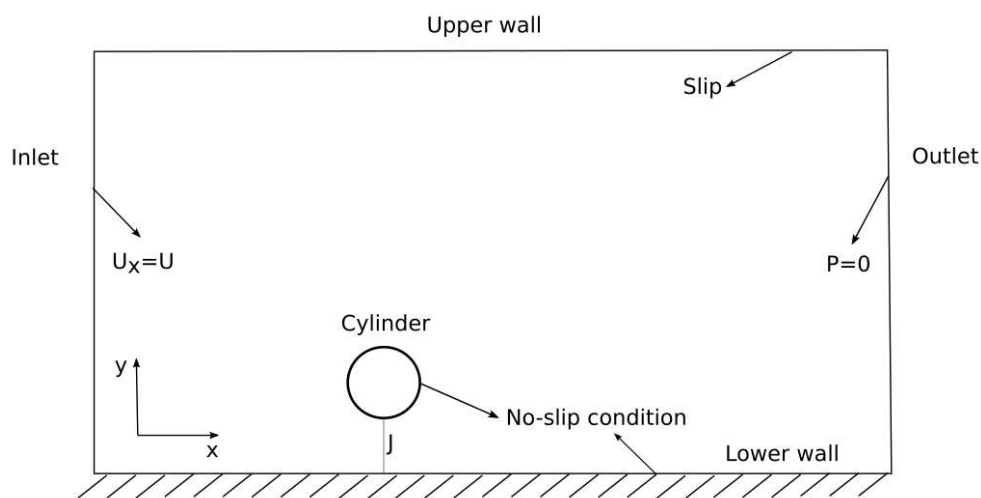


Figure 7: Schematic illustration for analyze seabed proximity

Cases with different gap ratio j/D values were simulated and the results of $\overline{C}d$, $\overline{C}l$, $\ddot{C}l$ and St for each case can be observed in Table 3.

$j(m)$	j/D	$\overline{C}d$	$\overline{C}l$	$\ddot{C}l$	St
0	0	0.59	0.36	0.016	0.05
0.25	0.5	0.94	0.07	0.005	0.09
0.5	1	1.167	0.003	0.018	0.1
0.75	1.5	1.32	0.08	0.18	0.15
5	10	1.36	0.02	0.33	1.67
10	20	1.339	0.007	0.345	0.167

Table 3: Comparison of hydrodynamic coefficients with the distance between the cylinder and seabed

It could be observed that when the cylinder was in the seabed, the values of $\overline{C}d$ and $\ddot{C}l$ varied significantly, as did the Strouhal number. As the ratio j/D increases, that is, there is the detachment of the cylinder from the lower wall, it begin to perceive the tendency of return of the values of the studied parameters to near the values of the base case, indeed it happens too.

It can also be observed from the values of $\overline{C}l$ that as j/D decreases, that is, the cylinder gets closer to the seabed, the asymmetry disappears, thus obtaining an mean lift coefficient increasingly distant from zero.

This can also be observed in the comparison between the horizontal velocity profile for such case studied. In Fig. 8 it is shown.

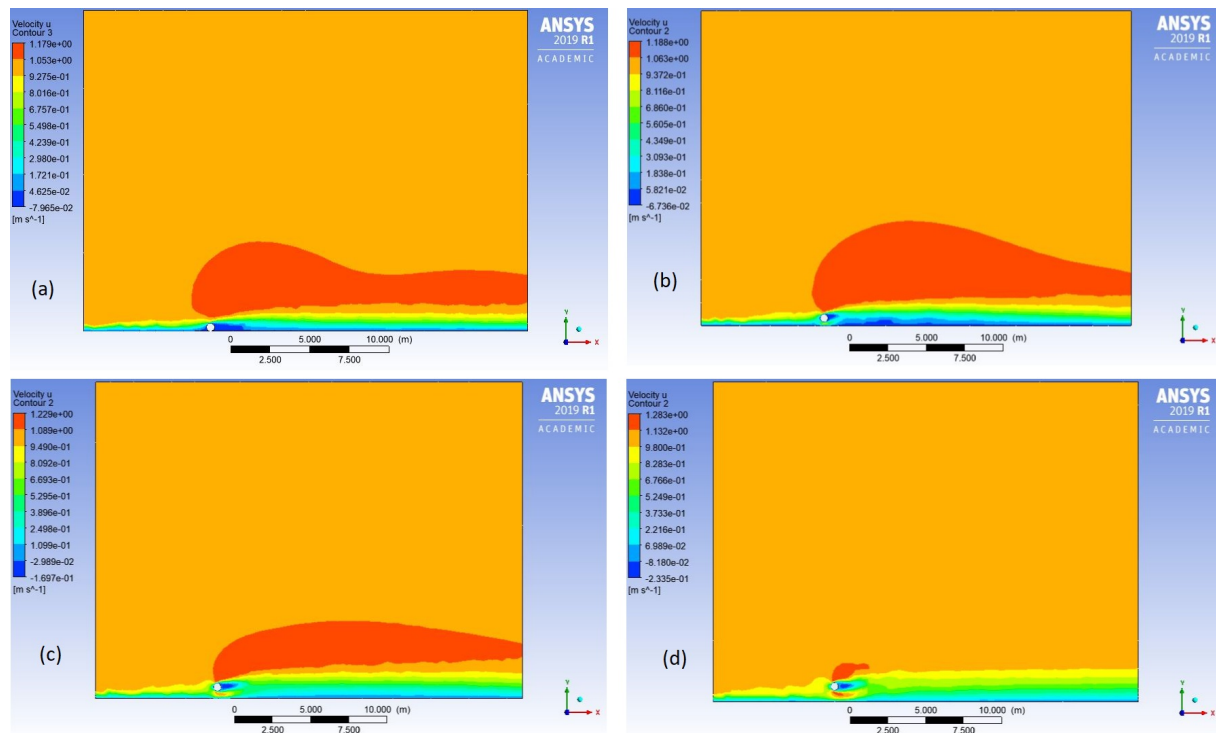


Figure 8: Horizontal velocity profile for (a) $j = 0$, (b) $j = 0.25$, (c) $j = 0.5$ and (d) $j = 0.75$

The experimental campaign from Bearman and Zdravkovich (1978) shown that the pressure distribution around the cylinder for small gaps was characterized by a displacement of the front stagnation point towards the gaps and by boundary layer thickness interaction from both cylinder and wall. The movement of the frontal stagnation point towards the wall is associated with the generation of an upward lift, while the movements of separation points with an increase of the base pressure result in a reduced drag coefficient (Sarkar and Sarkar, 2010). The lower shear layer of the cylinder is suppressed because of the wall boundary layer, which also affects the base pressure (Sarkar and Sarkar, 2010). This behavior could explain the lower values of $\overline{C_d}$ for $j/D = 0$.

4 CONCLUSIONS

The objective of this work was satisfactorily achieved. First, the values of $\overline{C_d}$, $\overline{C_l}$ and St for the base case converse perfectly well with experimental cases in the literature, as well as with other numerical cases in previous studies.

In this way, the Ansys Fluent model had satisfactory results when compared with other applied numerical methods in previous research and other software. The success of the results obtained in the first part of the research allowed the analysis of the second part, related to neighborhood effects and seabed proximity.

The analysis of neighborhood effects shown that the upstream cylinder (cylinder 1) is slightly influenced by the downstream cylinder (cylinder 2) for larger distance. In other words, there is a weak influence of wake. On the other hand, there is a strong influence of the upstream cylinder in the aerodynamic performance of the downstream cylinder.

Seabed proximity has huge influences in the aerodynamic performance of a singular cylinder. The closer as the cylinder is to the seabed, there is a suppression in vortex shedding and a loss of flow symmetry.

The results obtained in these analyses were what had hoped to obtain, and now as future work, we aim at increasing the Reynolds number and inserting models of turbulence in these analyzes. And with this, it will be possible to arrive at modeling closer to real cases of the offshore industry, like risers.

ACKNOWLEDGEMENTS

I thank the postgraduate program in computational modeling at the Federal University of Juiz de Fora and the Coordenação de Aperfeiçoamento de Pessoal de Nível Superior (CAPES) for all the structure and support available.

REFERENCES

- Abdulaziz M. *Study of the vortex-induced vibrations in off-shore structures*. Ph.D. thesis, Institute of Ship Technology, Ocean Engineering and Transport Systems (ISMT), 2017.
- Bearman P. and Zdravkovich M. Flow around a circular cylinder near a plane boundary. *Journal of Fluid Mechanics*, 89(1):33–47, 1978.
- Behr M., Hastreiter D., Mittal S., and Tezduyar T. Incompressible flow past a circular cylinder: dependence of the computed flow field on the location of the lateral boundaries. *International Journal for Numerical Methods in Engineering*, 123:309–316, 1995.
- Berthelsen P.A. and Faltinsen O.M. A local directional ghost cell approach for incompressible viscous flow problems with irregular boundaries. *International Journal for Numerical Methods in Engineering*, 227:4354–4397, 2008.
- Blazek J. *Computational Fluid Dynamics: Principles and Applications*, volume III. Elsevier, 2015.
- Cengel Y.A. and Cimbala J.M. *Fluid mechanics: Fundamentals and applications*, volume III. McGraw Hill, 2014.
- Dennis S. and Chang G. Numerical solutions for steady flow past a circular cylinder at reynolds numbers up to 100. *International Journal for Numerical Methods in Engineering*, 42:471–489, 1970.
- Mittal S. and Raghuvanshi A. Control of vortex shedding behind circular cylinder for flows at low reynolds numbers. *International Journal for Numerical Methods in Engineering*, 35:421–447, 2001.
- Sarkar S. and Sarkar S. Vortex dynamics of a cylinder wake in proximity to a wall. *Journal of Fluids and Structures*, 26(1):19–40, 2010.
- Stringer R., Zang J., and Hillis A. Unsteady rans computations of flow around a circular cylinder for a wide range of reynolds numbers. *International Journal for Numerical Methods in Engineering*, 87:1–9, 2014.
- Tawekal J.R. *CFD Simulation of the Flow over a 2-Dimensional Pipe and Vortex Induced Vibration of the Pipe with 1 Degree of Freedom*. Master's Thesis, University of Stavanger (UiS) - Faculty of Science and Technology, 2015.
- Tritton D. Experiments on the flow past a circular cylinder at low reynolds numbers. *International Journal for Numerical Methods in Engineering*, 6:547–567, 1959.